Cell Patterning Method on a Clinically Ubiquitous Culture Dish Using Acoustic Pressure Generated From Resonance Vibration of a Disk-Shaped Ultrasonic Transducer

Chikahiro Imashiro, Yuta Kurashina, Taiki Kuribara, Makoto Hirano, Kiichiro Totani, and Kenjiro Takemura, *Member, IEEE*

***Abstract*—Cell patterning methods have been previously reported for cell culture. However, these methods use inclusions or devices that are not used in general cell culture and that might affect cell functionality. Here, we report a cell patterning method that can be conducted on a general cell culture dish without any inclusions by employing a resonance vibration of a disk-shaped ultrasonic transducer located under the dish. A resonance vibration with a single nodal circle patterned C2C12 myoblasts into a circular shape on the dish with 10-min exposure of the vibration with maximum peak–peak amplitude of 10 $\mu m_{p\text{-}p}$. Furthermore, the relationship between the amplitude distribution of the transducer and the cell density in the patterned sample could be expressed as a linear function, and there was a clear threshold of amplitude for cell adhesion. To evaluate the cell function of the patterned cells, we conducted proliferation and protein assays at 120-h culture after patterning. Our results showed that the cell proliferation rate did not decrease and the expression of cellular proteins was unchanged. Thus, we conclude, this method can successfully pattern cells in the clinically ubiquitous culture dish, while maintaining cell functionality.**

***Index Terms*—Biotechnology, cell patterning, underwater ultrasound, ultrasonic transducer.**

Manuscript received March 13, 2018; accepted May 5, 2018. Date of publication May 14, 2018; date of current version December 19, 2018. This work was supported by the JSPS KAKENHI under Grant JP16H04259 and Grant JP17H07081; and in part by the MEXT Grant-in-Aid for the Program for Leading Graduate Schools. *(Corresponding author: Kenjiro Takemura.)*

C. Imashiro is with the School of Science for Open and Environmental Systems, Graduate School of Science and Technology, Keio University.

Y. Kurashina is with the Department of Mechanical Engineering, Faculty of Science and Technology, Keio University.

T. Kuribara and K. Totani are with the Department of Materials and Life Science, Faculty of Science and Technology, Seikei University.

M. Hirano is with the Department of Pharmacy, Yasuda Women's University.

K. Takemura is with the Department of Mechanical Engineering, Faculty of Science and Technology, Keio University, Kanagawa 223-8522, Japan (e-mail: takemura@mech.keio.ac.jp).

This paper has supplementary downloadable material available at http://ieeexplore.ieee.org.

Digital Object Identifier 10.1109/TBME.2018.2835834

I. Introduction

MULTIPLE biomedical engineering applications have been developed over the past several decades, including tissue engineering and organ-on-a-chip engineering [1], [2]. For these research applications, harvested human cells must be cultured in vitro to increase the number of cells. However, cells easily lose their functions in conventional culture [3], [4]. This loss of function is mainly caused by the difference in the culture environment compared with in vivo conditions. Thus, a cell culture method is required to maintain cell function in vitro for the purposes of maintaining cells for engineering applications.

Several techniques that mimic in vivo conditions have been previously reported [5], [6]. In these specific culture conditions, the culture medium, culture surface and cell–cell spatial relationships are all important factors [7]. However, from the viewpoints of fabricating tissue in vitro, establishing mechanical interaction between cells, and clarifying extracellular stimuli, the cell–cell spatial relationship is of critical importance to maintain cell function [8]. Many reports have demonstrated the importance of cell–cell spatial relationships in vitro. A previous study showed that muscle cells should be patterned lineally to regenerate skeletal muscles [9]. Furthermore, circularly patterned muscle cells could regenerate external anal sphincter muscles. In liver lobule tissue, hepatocytes are arranged into hexagonal or polygonal patterns [10]. Furthermore, the activity of cultured cells and stem cell differentiation rate are affected by the cell–cell spatial relationship [11]–[13]. Specifically, growth and differentiation of mouse embryoid bodies are highly affected by the patterned shape [14]. In addition, cell patterning is used in co-culture to observe the interaction of heterogeneous cells [15], [16]. Therefore, from basic to cutting edge techniques of biomedical engineering application, the development of cell patterning techniques has been important and the focus of recent research [17]–[19].

Many researchers have reported cell patterning methods using bio-printing, selective surface modification and magnetic force, among other approaches [20]–[23]. These methods can pattern cells into a desired shape, but there are still obstacles in widely using these techniques for a standard patterning method. The biggest challenge is the requirement for special, costly and

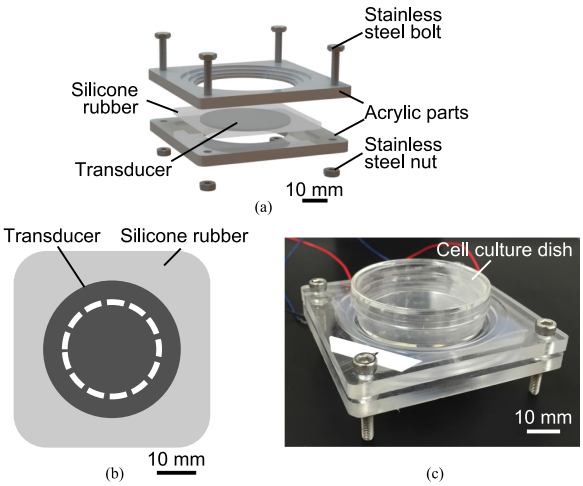

Fig. 1. The cell patterning device and the shape of node. (a) Enlarged view of the cell patterning device. (b) Image showing the nodal shape. (c) Picture of the cell patterning device. Scale bars, 10 mm.

time-intensive equipment [8], as, for example, most of the methods are not applicable in the clinically ubiquitous culture dish. In addition, the range of patterned shapes is quite limited. For example, a previously reported cell patterning technique involves a complex method that requires the use of oxygen plasma etching and elastomeric masks [24]. Furthermore, most of the methods require inclusions, such as collagen gel or magnetic particles, and these inclusions might affect cell functionality when used in biological applications [25]. Moreover, in some applications such as regenerative medicine employing cytokine therapy, the cell density must be kept high to effectively generate cytokines; however, some approaches involving collagen gel are unable to maintain high cell density [26], [27]. Furthermore, a complex device that is not disposable may also prove more time consuming and thus tedious for cell patterning, as each device must be sterilized in advance before use. Hence, a versatile, effective and simple method for patterning cells is required.

Acoustic vibrations may provide a potential solution to the obstacles in establishing the culture conditions. Acoustic vibrations generate an acoustic pressure gradient in cell suspension that enables cell patterning by trapping cells into the node/antinode area of pressure without any contact [28]–[31]. However, the method requires a special culture substrate, which is not acceptable in biomedical applications in practice. For practical use, cells should be cultured with a simple culture technique, maintaining sterile conditions and ensuring a consistent culture environment. Therefore, this research aims to develop a method to pattern cells in the clinically ubiquitous cell culture dish.

II. Materials and Methods

A. Cell Patterning Device

We fabricated a cell patterning device that can pattern cells in a standard culture dish; in this study, we performed cell patterning in a 35-mm cell culture dish (3000-035, AGC Techno Glass Co., Ltd., Shizuoka, Japan). As shown in Fig. 1(a), the cell patterning device is composed of a transducer embedded in silicone rubber, acrylic parts, stainless steel bolts and stainless steel nuts. The transducer has a resonance vibration with a single nodal circle to pattern cells into a circular shape, as shown in Fig. 1(b); this is the nodal shape of the primary resonance vibration mode of a disk. Note that the broken line in Fig. 1(b) shows the nodal position. When patterning cells, a 35-mm cell culture dish is placed on the transducer, as shown in Fig. 1(c). To effectively propagate vibration into the dish, the space between the cell culture dish and the transducer is filled with a substance whose acoustic impedance is equivalent to that of the material of a cell culture dish. Note that thickness of the space is 0.5 mm, which is defined by the shape of the dish. We used glycerol, which has an acoustic impedance of 2.43×10^6 N $\cdot$ s/m^3, which is similar (97.6%) to the material of the cell culture dish (polystyrene, 2.49×10^6 N $\cdot$ s/m^3). With this design, the vibration insonified from the transducer can directly propagate into the cell culture dish by simply placing the dish on this device.

The transducer is composed of a stainless steel disk (thickness: 1.0 mm, diameter: 35 mm) and a piezoelectric ceramic disk (thickness: 0.5 mm, diameter: 30 mm, C-213, Fuji Ceramics Corporation, Shizuoka, Japan). These are bonded to each other with epoxy adhesive (16223, Konishi, Osaka, Japan) under 3 N/m^2 pressure for 8 h. The dimension of the transducer was decided with reference to the 35-mm cell culture dish and the result of finite element analysis, shown in Supplementary Note 1.

B. Device Characterizations

We estimated the vibration characteristic of the transducer fabricated in this study. To measure the vibration amplitude, a laser Doppler vibrometer (CLV-3D, PI Polytech, Waldbronn, Germany) was used. The dish with 50-μL water was put on the device to simulate a cell patterning experiment. The color of the growth medium interfered with measurement using a laser Doppler vibrometer, so we used water instead of medium. The applicability is confirmed in Supplementary Note 2. To evaluate resonance vibration, maximum vibration amplitudes were measured at the center of the transducer, while changing the input frequencies with a driving voltage of 30 $V_{p\text{-}p}$. To identify the resonance vibration mode, we also evaluated the amplitude distribution with a driving voltage of 30 $V_{p\text{-}p}$ and a driving frequency at resonance. In short, equally spaced evaluation of the vibration amplitudes was conducted from the center to the edge on the transducer. Note that in this study we used continuous wave as an input signal.

C. Cell Preparation

The mouse myoblast cell line C2C12 (RCB0987, Riken Bio Resource Center, Ibaraki, Japan) was used to evaluate the proposed patterning method. Cells were cultured in growth medium (D-MEM/F12 (D8900, Sigma-Aldrich Co. LLC, MO, USA) supplemented with 10% fetal bovine serum (CELLect (TM) Gold, MP Biomedicals, Inc., CA, USA)) in a 5% CO2 humidified atmosphere incubator at 37 °C. Cell passage was performed

by trypsinization in 0.050% trypsin-EDTA (25300, Life Technologies, CA, USA) by pipetting.

D. Cell Patterning

Cultured cells were detached by trypsinization. Cells (2.0×10^5 cells/50-μL growth medium) were seeded into the dish, which was placed on the device as shown in Fig. 1(c) . Note that before seeding cells, the cell culture surface was washed with 1-mL growth medium to ensure the suspension spread on the dish, and the medium was removed soon after the washing. After seeding, the resonance vibration was excited on the transducer for 10 min in an incubator. The maximum peak-peak amplitudes of 5, 10 and 15 $\mu m_{p\text{-}p}$ were used, and the driving voltages were 20.78, 48.26 and 75.75 $V_{p\text{-}p}$, respectively. The driving frequency was set at the resonance. The driving signal pattern was continuous wave. After insonification of the vibration, the cell culture surface was washed twice with 500-μL growth medium, and 1-mL growth medium was added. As a control, we prepared samples following the same procedure but without any vibration. After these procedures, samples were incubated in an incubator.

After 24 h of culture, growth medium was removed, the cells were washed with 1-mL phosphate-buffered saline (PBS) twice, and differentiation medium (D-MEM/F12 supplemented with 5% horse serum (16050-122, Thermo Fisher Scientific, MA, USA)) was added. The patterned cells were then cultured for 96 h with daily replacement of differentiation medium. In total, samples were cultured for 120 h after the initial seeding.

E. Live Cell Detection

Live cells at 6-, 24-, 72- and 120-h culture after cell patterning were visualized by imaging. Cells were washed with PBS and incubated with 2-μL Calcein-AM (C396, Dojindo Molecular Technologies, MD, USA) in 1-mL serum-free medium for 30 min [32]. Fluorescence images were captured with an inverted fluorescence microscope (ECLIPSE Ti, Nikon Corporation, Tokyo, Japan) and these images were synthesized into a single large image of the entire dish with image synthesis software (NIS-Elements Documentation, Nikon Corporation, Tokyo, Japan).

F. Three-Dimensional Imaging

For observing the cross-section construction, cell nuclei and β-actin were stained with Hoechst33342 (Cellstain Hoechst33342 solution, Dojindo Molecular Technologies, MD, USA) and Rhodamine Phalloidin (R415, Thermo Fisher Scientific, MA, USA), respectively [33]. Cells were washed three times with PBS and then fixed with 2.5% glutaraldehyde in PBS for 20 min at room temperature. After three washes with PBS, cells were permeabilized with 0.1% Triton X-100 in PBS for 15 min, rinsed three times with PBS, and then blocked with 1% bovine serum albumin in PBS. Finally, cells were stained with 0.5% Hoechst33342 and 0.5% Rhodamine Phalloidin in blocking solution for 1 h at room temperature. Images were captured with a laser confocal microscope (Zeiss LSM 700 Confocal, Oberkochen, Germany).

G. Measuring Cell Distribution

Cell distribution was estimated by measuring cell densities with ImageJ (National Institutes of Health, Bethesda, MD, USA) [34]. We trimmed 3-mm-square areas around each position where vibration amplitudes were measured from the image of patterned cells, and the ratio of the area of the live cell to the area of the entire square was calculated as cell density. We performed this estimation for four directions radially from the center.

H. Cell Counting and Viability

Cell numbers at the seeding stage and after culturing were counted using a hemocytometer (A116, AS ONE, Osaka, Japan) under a phase contrast microscope (ECLIPSE Ti, Nikon Corporation, Tokyo, Japan). Trypsin was used for collecting cells, and Trypan blue (Gibco Trypan Blue Solution (0.4%), Thermo Fisher Scientific, MA, USA) was used to estimate cell viability.

I. Western Blot Analysis

Cells were lysed in sodium dodecyl sulfate polyacrylamide gel electrophoresis (SDS-PAGE) sample buffer (500 μL/1.0×10^5 cells). Samples were heated at 70 °C for 5 min and then separated by SDS-PAGE (7.5% Tris/HCl gel); proteins were then transferred onto polyvinylidene fluoride membranes by a transblotter for 2 h. The membranes were gently mixed with blocking one (Nacalai Tesque, Kyoto, Japan) for 1 h. The membranes were then incubated with primary antibodies: 2-μg/mL mouse anti-chicken myosin heavy chain (MHC) monoclonal antibody (MF20; R&D systems, Minneapolis, MN, USA), 0.4-μg/mL rabbit anti-human leukemia inhibitory factor receptor (LIFR) polyclonal antibody (22779-1-AP; Proteintech, Rosemont, IL, USA), or a 1,000-fold dilution of rabbit anti-mouse β-actin polyclonal antibody (#4967; Cell Signaling Technology, Boston, MA, USA) at 4 °C for 16 h. After washing with TBS containing 0.05% Tween 20 (TBS-T) (10 min, three washes), the membranes were incubated with secondary antibodies: a 10,000-fold dilution of horseradish peroxidase (HRP)-conjugated anti-mouse IgG (Sigma-Aldrich, St. Louis, MO, USA) or anti-rabbit IgG (Perkin-Elmer, Waltham, MA, USA) for 30 min with gentle shaking. After washing with TBS-T (10 min, three washes), the membranes were reacted with chemiluminescent reagent (Immobilon Western, Millipore). Protein bands were analyzed using a FluoroChemQ image analyzer (ProteinSimple, San Jose, CA, USA). The band density was normalized using the β-actin band and was expressed as the quantity relative to the control sample.

J. Statistical Analysis

The statistical significance of differences was evaluated by ANOVA with multiple comparison using Ryan's method. $P < 0.05$ or 0.01 was accepted as statistically significant.

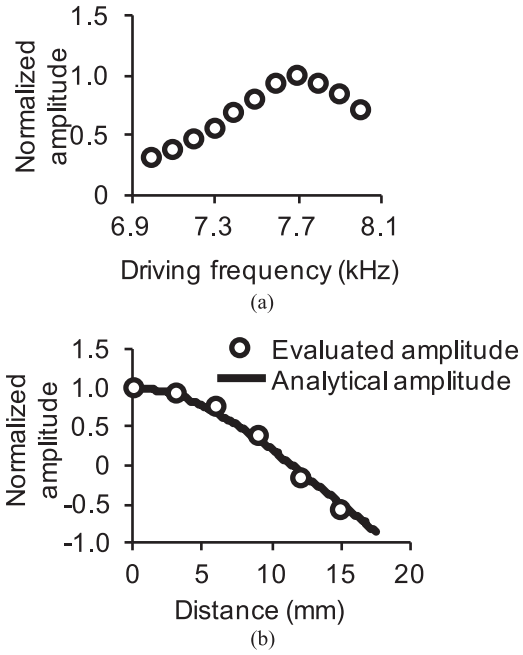

Fig. 2. Evaluation of the cell patterning device. The vibration amplitude was evaluated with a laser Doppler vibrometer. The amplitude was normalized by the maximum amplitude and the driving voltage was 30 $V_{p\text{-}p}$. (a) Relationship between driving frequency and normalized amplitude. (b) Comparison of the evaluated and the analytical amplitude distribution that is a relationship between the distance from the center of the culture substrate and cell densities with resonance.

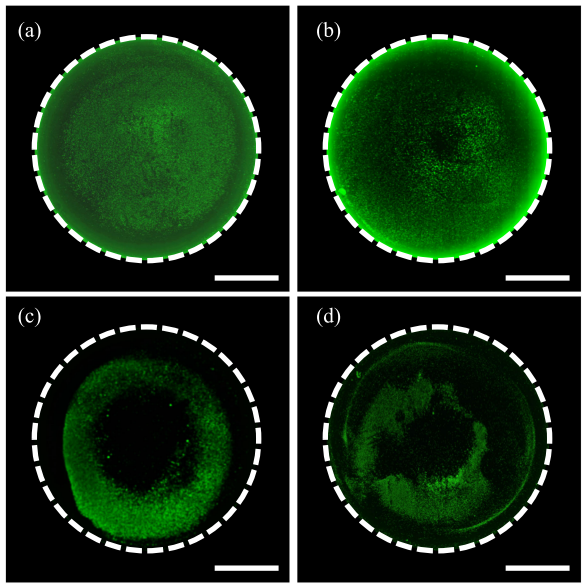

Fig. 3. Fluorescent images of the cell patterning results with (a) the control or a maximum amplitude of (b) 5 $\mu m_{p\text{-}p}$, (c) 10 $\mu m_{p\text{-}p}$, or (d) 15 $\mu m_{p\text{-}p}$. The number of seeded cells was 2.0×10^5 and patterned cells were cultured for 6 h. Live cells were dyed with Calcein-AM. The broken line shows the edge of the dish.

III. Result

A. Estimation of Resonance Frequency and Vibration Amplitude Distribution

Fig. 2 shows the resonance frequency and vibration amplitude distribution of the resonance vibration. Fig. 2(a) shows the relationship between the driving frequency and the maximum amplitude with a driving voltage of 30 $V_{p\text{-}p}$. Note that the amplitude was normalized to the maximum value. From Fig. 2(a), the resonance frequency at 7.7 kHz was identified, where the amplitude was the highest. Additionally, in Fig. 2(b), the vibration amplitude distribution at resonance was estimated and compared with the value from the analysis obtained in Supplementary Note 1. Note that the experiment was conducted with a driving voltage of 30 $V_{p\text{-}p}$ and driving frequency of 7.7 kHz. Because the evaluated amplitudes correspond to the analytical data, the Fig. 2(b) results show that the resonance vibration with single nodal circle has successfully been excited.

B. Cell Distribution

We next captured live cell images of patterned cells after 6-h incubation (Fig. 3). We found a relationship between the cell distribution and the maximum vibration amplitude. Additionally, these images allowed us to estimate cell distributions. To qualitatively estimate the cell patterning, we showed the comparison of the vibration amplitude and the cell distribution in Figs. 4(a)–(d). Furthermore, Figs. 4(e)–(g) show the relationship between the vibration amplitude and the cell density with each vibrational condition. When the resonance vibration with maximum amplitude of 10 $\mu m_{p\text{-}p}$ was excited, the vibration amplitude and the cell density have a relation of monotone decreasing from the nodal position to the position with 5 $\mu m_{p\text{-}p}$ vibration amplitude, as shown in Fig. 4(f). This indicates that the resonance vibration with maximum amplitude of 10 $\mu m_{p\text{-}p}$ was proper for cell patterning in the proposed method. In Fig. 4(f) with the proper vibration, linear regression was conducted using the data with amplitudes of about 5.0 $\mu m_{p\text{-}p}$ and lower, because the threshold amplitude for cell adhesion is around 5.0 $\mu m_{p\text{-}p}$ in this cell patterning method.

The patterned and control samples were then cultured for 120 h to estimate the effect of the proposed method on cell viability and functionality. Figs. 5(a) and (b) show images of live cells cultured for 120 h after the initial seeding. In the control sample, cells were spread all over the dish. In contrast, the patterned cells proliferated in a circular shape, which corresponds to the nodal shape at the resonance. The images at 24- and 72-h culture are shown in Supplementary Fig. 3.

We also measured the temperature variation of the medium when exciting vibration. Supplementary Fig. 4 shows the temperature variation of the medium as a function of time, and we concluded that fatal temperature variation did not occur in each condition [35].

C. Proliferation Assay

We next evaluated cell proliferation by calculating the numbers of patterned and control cells after 6-, 24-, 72-, and 120-h culture [Fig. 5(c)]. After 6 h, the number of control cells was significantly higher than that of patterned cells, but the

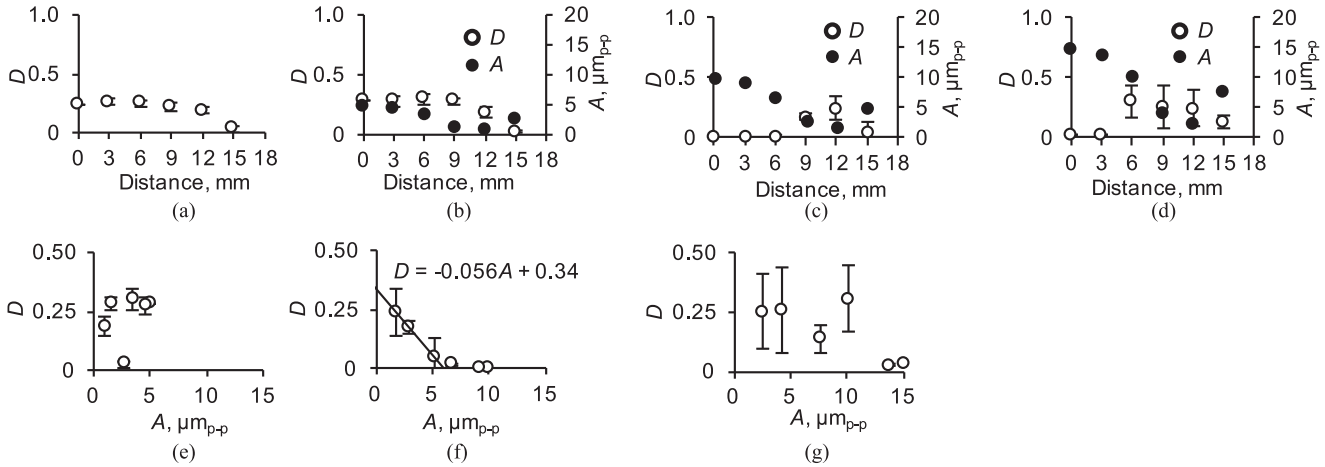

Fig. 4. (a) Cell patterning results of the control cells and cells with a maximum amplitude of (b) and (e) 5 μm$_{p\text{-}p}$, (c) and (f) 10 μm$_{p\text{-}p}$, and (d) and (g) 15 μm$_{p\text{-}p}$ (mean $\pm$ SD, $n = 4$). (a)–(d) Comparison of the amplitude distribution and the cell distribution. (e)–(g) Relationship between the vibration amplitude, A, and the cell density, D. The number of seeded cells was 2.0×10^5 and patterned cells were cultured for 6 h. The ratio of the area of live cells to the area of the entire square was calculated as cell density.

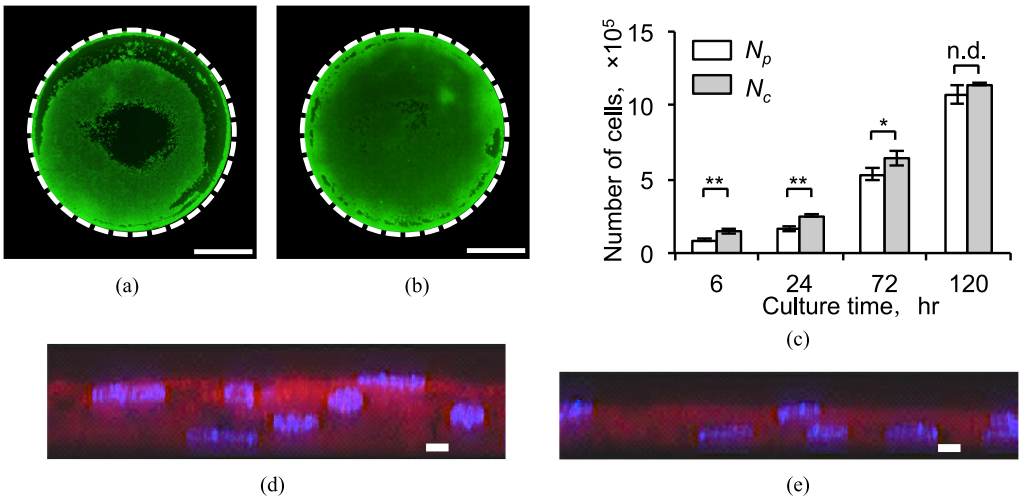

Fig. 5. Patterned and control samples with 120-h culture after seeding. (a) and (b) Fluorescent images of patterned and control samples, respectively. Live cells were dyed with Calcein-AM. Scale bars indicate 10 mm. The broken line shows the edge of the dish. (c) Proliferation of the samples (mean $\pm$ SD, $n = 4$, $^{*}p < 0.05$, $^{**}p < 0.01$). N_p: Number of patterned cells. N_c: Number of control cells. (d) and (e): Cross-section images of patterned and control samples, respectively. Cell nuclei and β-actin were stained with Hoechst33342 (blue) and Rhodamine Phalloidin (red), respectively. Scale bars indicate 10 μm.

differences between pattern and control cell numbers became reduced over culture time. After 120-h culture, there was no statistically significant difference between the two groups. Together these data indicate that vibration does not decrease cell proliferation. Furthermore, we assayed the activity of the cells that did not attach to the dish after the experiment and did not detect any dead cells.

D. Three-Dimensional Structure of Samples

We next examined the three-dimensional structure of the samples (Figs. 5(d) and (e)). The cross-section images of patterned and control cells were generated by accumulating a number of confocal microscopic images. These images were captured at 12 mm away from the center of the culture dish, corresponding to the nodal position, and processed with ZEN lite Ver.2.3 (Carl Zeiss). These data show stacking and overlapping of the nuclei in the patterned cells, indicating that the patterned cells pile up on each other. In contrast, the control cells maintained culture in a single layer.

E. Expression of Membrane and Intracellular Proteins

To estimate the effect of the cell patterning method on cell functionality, we quantified membrane and intracellular proteins in pattered and control cells using western blot analysis [Fig. 6(a)]. For evaluating membrane and intracellular proteins, we choose leukemia inhibitory factor receptor (LIFR) and myosin heavy chain (MHC), respectively. MHC is an index of differentiation rate and LIFR is related to differentiation [36].

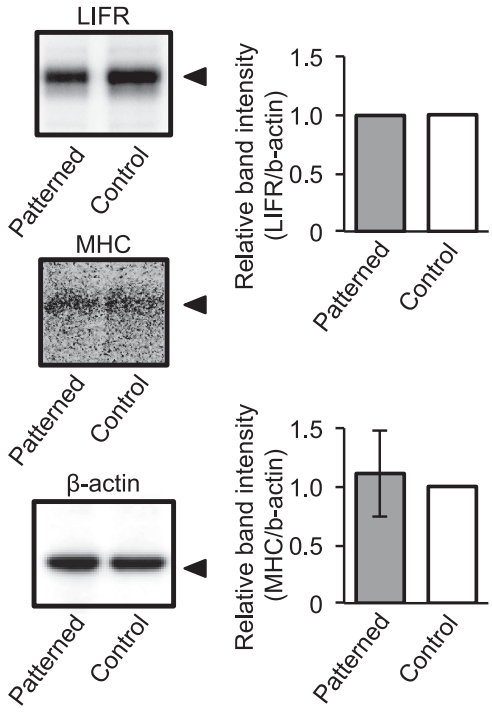

Fig. 6. Western blot analysis of C2C12 cells. (a) Western blot of patterned and control cells using anti-leukemia inhibitory factor receptor (LIFR, top panel), anti-myosin heavy chain (MHC) (middle panel), and anti-β-actin (bottom panel) antibodies. Arrows indicate the target protein bands. (b) Relative protein quantities of LIFR and MHC were measured using their band densities on western blots. Protein quantities were normalized to the band density of β-actin. The data are expressed as means with standard deviation ($n = 3$).

β-Actin was used as loading control. Quantification of the protein levels, shown in Fig. 6(b), revealed no changes in the quantity of the two selected proteins between the two groups. These results indicate that the resonance vibration does not generate damage to membrane and intracellular proteins and has no effect on the cellular differentiation rate.

IV. Discussion

In this study, we demonstrate a novel cell patterning method using a clinically ubiquitous cell culture device by resonance vibration of a disk-shaped transducer. The proposed method can pattern cells on a cell culture dish into the corresponding nodal shape of the resonance vibration, as shown in Fig. 3. Additionally, we confirmed that cell functionality was not impacted by our method.

Figs. 3 and 4 reveal a suitable maximum amplitude of vibration, 10 $\mu m_{p\text{-}p}$, for cell patterning. When we applied a low vibration amplitude with a maximum amplitude of 5 $\mu m_{p\text{-}p}$, the cell distribution was not changed from the control, indicating that the maximum vibration amplitude of 5 $\mu m_{p\text{-}p}$ was too small to generate enough acoustic pressure for cell patterning in our experiment. In contrast, acoustic streaming was induced by the resonance vibration with a maximum amplitude of 15 $\mu m_{p\text{-}p}$, which prevents cell patterning. Furthermore, as shown in Fig. 4(f), the relationship between the vibration amplitude distribution and the cell density could be expressed by the linear function, and there is a vibration amplitude threshold in which cells cannot adhere.

Fig. 4(c) and (f) may not show a perfect match between the vibration amplitude distribution and the cell distribution. One explanation may be that 2.0×10^5 cells were included in the medium in this experiment, and the movement of cells was affected by neighboring cells. Thus, the shapes of the patterned cells did not exactly correspond to the nodal shape of the resonance vibration.

To control acoustic streaming, we used 50-μL culture medium in cell patterning, because the strength of acoustic streaming is related to the height of medium [37]. Actually, as shown in Supplementary Fig. 5 with experimental results using 1-mL medium, the relationship between the cell distribution and vibration amplitude distribution could not be expressed by the linear function. This indicates that cell patterning by resonance vibration could not be conducted with 1-mL medium, which is the standard condition for culture.

Using a low, kHz order, frequency vibration allows for cells to be patterned on a cell culture dish entirely with acoustic pressure generated by a resonating transducer. In previous studies, cells were patterned with high frequency vibration, e.g., MHz order, resulting in patterning cells in the limited area of the special device, because the attenuation coefficient regarding vibration propagation is proportional to the square value of frequency [38]. Thus, the previous method rendered it difficult to pattern cells on a cell culture dish entirely by the incoming vibration from outside of the dish. Vibration from the transducer can then efficiently propagate into a cell culture dish by kHz order vibration. In almost all of the studies on cell patterning using vibration, MHz range vibrations are used because the acoustic pressure depends on frequency and amplitude [39]. Therefore, to obtain enough acoustic pressure for cell patterning with low frequency vibration, large amplitude vibration must be acquired. We achieved this requirement by introducing the out-of-plane resonance vibration mode of the disk-shaped transducer.

In many of the cell patterning methods that use vibration, the shapes of cell patterning have been limited to the combination of straight lines. The reason for this limitation is the use of an acoustic pressure gradient. The gradient is due to the node/anti-node generation of standing wave of culture medium. In comparison, resonance vibrations of an elastic body have infinite nodal/anti-nodal shapes corresponding to the resonance frequency depending on the shape of the body [40]. Additionally, there are infinite nodal shapes of resonance vibrations, some of which are shown in Supplementary Fig. 6. Therefore, cells could be pattered into other shapes by using other resonance modes just by changing the driving frequencies. As shown in Supplementary Fig. 7, we confirmed that cells were successfully patterned into another pattern. This indicates that our proposed method will allow the patterning of cells into several shapes in a cell culture dish just by changing the driving frequency. The vibration amplitude should be modulated with each resonance frequency. However, if we use a higher frequency, we should use a lower vibration amplitude. This is because the cell patterning is conducted by acoustic pressure, which is expressed

by monotonically increasing function of vibration frequency and amplitude [41].

Our method has demonstrated successful cell patterning of C2C12 cells. However, for successful use of the patterned cells in biomedical applications, cell functionality must be maintained before and after the patterning. We thus also conducted cell function assays in this study. Proliferation assays did not reveal any significant difference in number of cells between the patterned and control samples at 120-h culture after cell patterning, although the number of control cells was larger than the number of patterned cells soon after cell patterning. Further, no dead cells were detected in the experiment. This indicates that vibration prevented cell adhesion, but did not negatively impact or diminish cellular activity, such as proliferation.

Interestingly, as shown in Figs. 5(a)–(c), although the area of live cells was different between the patterned and the control samples, almost the same number of cells were observed. One reason for this observation is shown in the cross-section images, which show thicker patterned samples compared with control samples. This thicker structure is caused by two reasons. First, because cells were rapidly gathered into the nodal circle with our device, cells have less time for differentiation, which is caused by cell–cell contact and decreases cell proliferation [41], [42]. Cells then continuously proliferated at a high cell density, resulting in a thicker structure. Second, the patterned sample shrunk because of the intercellular tension and the stacking of the cells. Cells have intercellular tension [43]. The cultured control cells spread over the cell culture dish, without sample shrinking or cell stacking, indicating each cell was subjected to intercellular tension from all directions. In contrast, in the patterned sample, there is the nodal area on which cells can adhere and the antinodal area on which cells can not adhere, indicating that cells around the boundary between the nodal area and the antinodal area are subjected to intercellular tension from the direction toward the node position. Due to this directional tension, the patterned sample shrunk and generated a three-dimensional structure.

To determine whether the proposed cell patterning method had any effect on cell function, we also evaluated the expressions of MHC, LIFR and β-actin proteins. MHC and β-actin are intracellular proteins, whereas LIFR is a membrane protein. MHC and LIFR are related to the differentiation rate of C2C12 myoblasts, whereas β-actin is a stable protein and is commonly used as a loading control in many studies. No changes in expression were detected for these proteins, which range in cellular characteristics and function, indicating that cell functionality was not impacted by our method. One reason for evaluating the differentiation rate is that some stimuli, including vibration stimuli, have been used to induce differentiation of C2C12 cells [44], [45]. Our results demonstrated that our method effectively generated patterned cells, and the characteristics and viability of these pattern cells were not altered or decreased by the proposed method, as shown by proliferation and protein assays.

Together these results show that our 10-min insonification method can pattern cells with no effect on cell functionality. Therefore, we conclude that the proposed method can successfully pattern cells on the clinically ubiquitous cell culture dish. In short, we developed a simple, label-free, contact-free and flexible cell patterning method that allows for extended culture and reduced risk for contamination.

In many of the studies on cell patterning, cells could not be observed sequentially with a phase-contrast microscope and cell conditions, such as proliferation and protein expression, could not be evaluated after patterning, because it is difficult to create and maintain sterile conditions in the device [15]. Thus, the effect of vibration on cells with long period culture after patterning was not evaluated in previous studies. In this research, as our method patterned cells on a cell culture dish, the cell functionality of patterned cells can easily be evaluated. Furthermore, our method allows observation of the generation of three-dimensional cell tissue during long periods of culture. This method allows researchers to pattern cells into several shapes, and the relationship between the shape of cell patterning and the cell functionality could be studied to determine the best shape for each cell type and application. The cell patterning technique using resonance vibration could be a promising method for cell patterning because this is the first technique to pattern cells on a cell culture dish with no inclusion. Importantly, our patterning method could be used for therapy because of sterile conditions and the absence of impact on cell functionality. We believe that this technique could contribute to the development of novel regenerative medicine applications.

V. Conclusion

In this study, we proposed a novel method for patterning cells in a clinically ubiquitous culture dish by using an acoustic pressure generated from a resonating disk-shaped ultrasonic transducer. The developed cell patterning device can pattern cells corresponding to the nodal shape of resonance vibration of the transducer. This is the first technique to pattern cells on a culture dish with no inclusion, not providing any effect on cell functionality even after 120-h culture with 10-min patterning. Thus this technique using acoustic pressure could be a promising method for cell patterning.

Acknowledgment

The authors have no conflict of interest to declare.

References

[1] R. Langer and J. P. Vacanti, "Tissue engineering," *Science*, vol. 260, no. 5110, pp. 920–926, May 1993.
[2] H. Lee *et al.*, "A pumpless multi-organ-on-a-chip (MOC) combined with a pharmacokinetic-pharmacodynamic (PK-PD) model," *Biotechnol. Bioeng.*, vol. 114, no. 2, pp. 432–443, Feb. 2017.
[3] A. Guillouzo. "Liver cell models in in vitro toxicology," *Environ. Health Perspect*, vol. 106, pp. 511–532, Apr. 1998.
[4] W. Thorsten *et al.*, "The potential of bioartificial tissues in oncology research and treatment," *Onkologie*, vol. 30, pp. 388–394, Jun. 2007.
[5] I. Kuzin *et al.*, "Long-term immunologically competent human peripheral lymphoid tissue cultures in a 3D bioreactor," *Biotechnol. Bioeng.*, vol. 108, no. 6, pp. 1430–1440, Jun. 2011.
[6] A. B. Yeatts *et al.*, "Human mesenchymal stem cell position within scaffolds influences cell fate during dynamic culture," *Biotechnol. Bioeng.*, vol. 109, no. 9, pp. 2381–2391, Sep. 2012.
[7] T. Chen *et al.*, "Engineering superficial zone features in tissue engineered cartilage," *Biotechnol. Bioeng.*, vol. 110, no. 5, pp. 1476–1486, May 2013.

[8] F. Gesellchen *et al.*, "Cell patterning with a heptagon acoustic tweezer – application in neurite guidance.," *Lab Chip*, vol. 19, pp. 2266–2275, Apr. 2014.

[9] M. T. Lam *et al.*, "The effect of continuous wavy micropatterns on silicone substrates on the alignment of skeletal muscle myoblasts and myotubes," *Biomaterials*, vol. 27, no. 24, pp. 4340–4347, Aug. 2006.

[10] C. T. Ho *et al.*, "Liver-cell patterning lab chip: Mimicking the morphology of liver lobule tissue," *Lab Chip*, vol. 13, no. 18, pp. 3578–3587, Sep. 2013.

[11] S. M. Chambers *et al.*, "Highly efficient neural conversion of human ES and iPS cells by dual inhibition of SMAD signaling," *Nat. Biotechnol.*, vol. 27, no. 3, pp. 275–280, Mar. 2009.

[12] K. Nakazawa *et al.*, "Effect of cell spot sizes on micropatterned cultures of rat hepatocytes," *Biochem. Eng. J.*, vol. 53, no. 1, pp. 85–91, Dec. 2010.

[13] K. Nakazawa *et al.*, "Effects of culture conditions on a micropatterned co-culture of rat hepatocytes with 3T3 cells," *J. Bioprocess. Biotech.*, vol. 1, no. 3, pp. 1–5, Aug. 2011.

[14] D. Miyamoto *et al.*, "Effect of separation distance on the growth and differentiation of mouse embryoid bodies in micropatterned cultures," *J. Biosci. Bioeng.*, vol. 121, no. 1, pp. 105–110, Jan. 2016.

[15] C. Cho *et al.*, "Layered patterning of hepatocytes in co-culture systems using microfabricated stencils," *Biotechniques*, vol. 48, no. 1, pp. 47–52, Jan. 2010.

[16] S. Kidambi *et al.*, "Patterned Co-Culture of primary hepatocytes and fibroblasts using polyelectrolyte multilayer templates," *Macromol. Biosci.*, vol. 7, no. 3, pp. 344–353, Mar. 2007.

[17] A. Ashkin *et al.*, "Optical trapping and manipulation of single cells using infrared laser beams," *Nature*, vol. 330, no. 6150, pp. 769–771, Dec. 1987.

[18] M. S. Kim *et al.*, "Microvalve-assisted patterning platform for measuring cellular dynamics based on 3D cell culture," *Biotechnol. Bioeng.*, vol. 101, no. 5, pp. 1005–1013, Dec. 2008.

[19] R. S. Thomas *et al.*, "Negative DEP traps for single cell immobilisation," *Lab Chip*, vol. 9, no. 11, p. 1534, Jun. 2009.

[20] M. N. De Silva *et al.*, "Two-step cell patterning on planar and complex curved surfaces by precision spraying of polymers," *Biotechnol. Bioeng.*, vol. 93, no. 5, pp. 919–927, Apr. 2006.

[21] K. Ino *et al.*, "Application of magnetic force-based cell patterning for controlling cell-cell interactions in angiogenesis," *Biotechnol. Bioeng.*, vol. 102, no. 3, pp. 882–890, Feb. 2009.

[22] D. Nofziger and G. Weinmaster, "Notch signaling imposes two distinct blocks in the differentiation of C2C12 myoblasts," *Development*, vol. 126, pp. 1689–1702, Apr. 1999.

[23] I. Paik *et al.*, "Rapid micropatterning of cell lines and human pluripotent stem cells on elastomeric membranes," *Biotechnol. Bioeng.*, vol. 109, no. 10, pp. 2630–2641, Apr. 2012.

[24] A. Tourovskaia *et al.*, "Micropatterns of chemisorbed cell adhesion-repellent films using oxygen plasma etching and elastomeric masks," *Langmuir*, vol. 19, no. 11, pp. 4754–4764, May 2003.

[25] Y. Liu *et al.*, "In vitro construction of scaffold-free bilayered tissue-engineered skin containing capillary networks," *Biomed Res. Int.*, vol. 8, 2013.

[26] H. Nakagami *et al.*, "Adipose tissue-derived stromal cells as a novel option for regenerative cell therapy," *J. Atheroscler. Thromb.*, vol. 13, no. 2, pp. 77–81, Apr. 2006.

[27] Y. Sawa and S. Miyagawa, "Present and future perspectives on cell sheet-based myocardial regeneration therapy," *Biomed Res. Int.*, vol. 2013, pp. 583912, Dec. 2013.

[28] F. Guo *et al.*, "Controlling cell-cell interactions using surface acoustic waves," in *Proc. Natl. Acad. Sci. USA*, Nov. 2015, vol. 112, no. 1, pp. 43–48.

[29] K. H. Lam *et al.*, "Ultrahigh frequency lensless ultrasonic transducers for acoustic tweezers application," *Biotechnol. Bioeng.*, vol. 110, no. 3, pp. 881–886, Mar. 2013.

[30] C. Imashiro *et al.*, "Cell patterning method using resonance vibration of a metallic cell cultivation substrate," *Adv. Biomed. Eng.*, vol. 5, pp. 142–148, Dec. 2016.

[31] J. Lee *et al.*, "Targeted cell immobilization by ultrasound microbeam," *Biotechnol. Bioeng.*, vol. 108, no. 7, pp. 1643–1650, Jul. 2011.

[32] K. Sumaru *et al.*, "On-demand killing of adherent cells on photo-acid-generating culture substrates," *Biotechnol. Bioeng.*, vol. 110, no. 1, pp. 348–352, Aug. 2013.

[33] F. Wada *et al.*, "Analyses of expression and localization of two mammalian- type transglutaminases in Physarum polycephalum, an acellular slime mold," *J. Biochem.*, vol. 136, pp. 665–672, Nov. 2004.

[34] J. Kandel *et al.*, "Automated detection of whole-cell mitochondrial motility and its dependence on cytoarchitectural integrity," *Biotechnol. Bioeng.*, vol. 112, no. 7, pp. 1395–1405, Mar. 2015.

[35] E. Mitri *et al.*, "Time-resolved FT-IR microspectroscopy of protein aggregation induced by heat-shock in live cells," *Anal. Chem.*, vol. 87, no. 7, pp. 3670–3677, Mar. 2015.

[36] Y. Kurashina *et al.*, "Enzyme-free cell detachment mediated by resonance vibration with temperature modulation," *Biotechnol. Bioeng.*, vol. 114, no. 10, pp. 2279–2288, Oct. 2017.

[37] R. J. Shilton *et al.*, "Nanoliter-droplet acoustic streaming via ultra high frequency surface acoustic waves," *Adv. Mater.*, vol. 26, no. 29, pp. 4941–4946, Mar. 2014.

[38] M. C. Domingo. "Overview of channel models for underwater wireless communication networks," *Phys. Commun.*, vol. 1, no. 3, pp. 163–182, Sep. 2008.

[39] D. Collins *et al.*, "Continuous micro-vortex-based nanoparticle manipulation via focused surface acoustic waves," *Lab Chip*, vol. 17, no. 1, pp. 91–103, Jan. 2017.

[40] X. Shi *et al.*, "A unified method for free vibration analysis of circular, annular and sector plates with arbitrary boundary conditions," *J. Vib. Control*, vol. 22, no. 2, pp. 442–456, May 2014.

[41] S. L. Nedelec *et al.*, "Particle motion: the missing link in underwater acoustic ecology," *Methods. Ecol. Evol.*, vol. 7, no. 7, pp. 836–842, Jul. 2016.

[42] P. Diel *et al.*, "C2C12 myoblastoma cell differentiation and proliferation is stimulated by androgens and associated with a modulation of myostatin and Pax7 expression," *J. Mol. Endocrinol.*, vol. 40, no. 5–6, pp. 231–241, May 2008.

[43] A. S. T. Smith *et al.*, "Characterization and optimization of a simple, repeatable system for the long term in vitro culture of aligned myotubes in 3D," *J. Cell. Biochem.*, vol. 113, no. 3, pp. 1044–1053, Mar. 2012.

[44] S. Ding *et al.*, "Modulation of human mesenchymal and pluripotent stem cell behavior using biophysical and biochemical cues: A review," *Biotechnol. Bioeng.*, vol. 114, no. 2, pp. 260–280, Feb. 2017.

[45] B. D. Riehl *et al.*, "Mechanical stretching for tissue engineering: two-dimensional and three-dimensional constructs," *Tissue Eng. Part B. Rev.*, vol. 18, no. 4, pp. 288–300, Aug. 2012.

[46] Y. Zhang *et al.*, "Binding of carbon nanotube to BMP receptor 2 enhances cell differentiation and inhibits apoptosis via regulating bHLH transcription factors," *Cell Death Dis*., vol. 3, p. e308, May 2012.